Interpretation of the Photoluminescence Decay Kinetics in Metal Halide Perovskite Nanocrystals and Thin Polycrystalline Films

Vladimir S. Chirvony,[1]* Kairolla S. Sekerbayev,[2] Hamid Pashaei Adl,[1] Andrés F. Gualdrón-Reyes,[3] Iván Mora-Seró,[3] Juan P. Martínez-Pastor[1]

[1]UMDO (Unidad de Materiales y Dispositivos Optoelectrónicos), Instituto de Ciencia de los Materiales, Universidad de Valencia, Valencia 46071, Spain;[2]Institute of Experimental and Theoretical Physics, Al-Farabi Kazakh National University, Almaty, 050040 Kazakhstan; *[3]Institute of Advanced Materials (INAM), Universitat Jaume I, Castelló 12006, Spain*

Abstract

One of distinguishing features of metal halide perovskites is their long (up to microseconds) photoluminescence (PL) lifetimes, which are regularly observed for this class of semiconductors in spite of their direct gap origin. It is difficult to explain this contradiction in the framework of usual two-level Jablonski photophysical diagram because the absorption coefficient (i.e., the oscillator strength of the direct optical transition) is too high in perovskites to hold such long PL lifetimes. In this paper, we describe practical steps how the PL decay kinetics of perovskites in the forms of (1) passivated nanocrystals and (2) thin multicrystalline films can be described. In case of nanocrystals, the three-level delayed luminescence model is described by including shallow non-quenching traps providing multiple trapping and de-trapping of carriers and thus essentially lengthening the observed PL lifetime. In the case of perovskite thin films limited by interfacial recombination, the PL decay kinetics is usually determined by the non-radiative recombination on the film surfaces and can be satisfactorily described in terms of one-dimensional diffusion equation. The limits of applicability of such approaches are discussed.

Introduction

Metal halide perovskites (hereinafter perovskites) in all their forms (nanocrystals, thin films of microcrystals, single crystals) demonstrate a large variety of the photoluminescence (PL) lifetimes. In particular, in case of perovskite thin films and nanocrystals the PL decay times span over more than 3 orders of magnitude, from about one nanosecond to more than several microseconds [1-4]. Besides, far from always the PL lifetimes correlate with quantum yields (QY), especially in the case of nanocrystals: formally same nanocrystals produced in different laboratories demonstrate orders of magnitude different PL lifetimes with comparable PLQY [5-7]. Moreover, PL lifetime of the same nanocrystals can depend on the degree of their aggregation [6]. The abundance of experimental results in the field of perovskite photophysics not only does not help to understand how the PL kinetics is formed in this class of compounds, but rather complicates a reliable interpretation, mainly due to contradictory conclusions made by different authors. In this work, we describe practical approaches how one can interpret PL decay kinetics for most widely investigated metal halide perovskite structures, such as nanocrystals with well passivated surfaces and thin polycrystalline films. In the first case, the contradiction between the observed long PL lifetimes and the expected short exciton radiative lifetime (high radiative recombination rate determined by its high absorption cross section) in perovskites is overcome by means of a three-level energy diagram including shallow non-quenching traps, as a reason of the PL kinetics retardation. In the second case, the non-radiative recombination at the film surfaces is shown to be the process mostly contributing to the PL decay kinetics, which can be satisfactorily described in terms of one-dimensional diffusion equation enabling determination of the diffusion coefficient D and the surface recombination velocity S. As far as the single perovskite crystals is concerned,

they will not be considered here because their PL kinetics is strongly influenced by the PL reabsorption in bulk which in turn depends on excitation/detection experimental conditions [8, 9].

PL decay kinetics in perovskite nanocrystals

In terms of phenomenological photophysics, the PL decay kinetics of perovskite nanocrystals is always considered in literature in the framework of a two-level diagram including the ground (unexcited) and excited states (the states 0 and 1 in Fig. 1a) and radiative and non-radiative deactivation channels (solid and dashed lines, rate constants k_r and k_{nr}, respectively). Within this diagram, the simple phenomenological formulas (1) and (2) link the PL lifetime τ_{PL} and the quantum yield Φ with the radiative and non-radiative rate constants:

$$\tau_{PL} = \frac{1}{k_r + k_{nr}} \quad (1)$$

$$\Phi = \frac{k_r}{k_r + k_{nr}} \quad (2)$$

Following this approach, the values of k_r and k_{nr} can be easily calculated on the basis of the experimentally measurable τ_{PL} and Φ values. As an easy numerical example, if we suppose τ_{PL} = 25 ns and Φ = 1.0 (it results in $k_r = (25\ \text{ns})^{-1} = 4 \cdot 10^7\ \text{s}^{-1}$ and $k_{nr} = 0$) and then introduce some non-radiative process which decreases PL lifetime and PLQY down to 12.5 ns and 0.5, respectively, it results in $k_r = k_{nr} = (25\ \text{ns})^{-1} = 4 \cdot 10^7\ \text{s}^{-1}$.

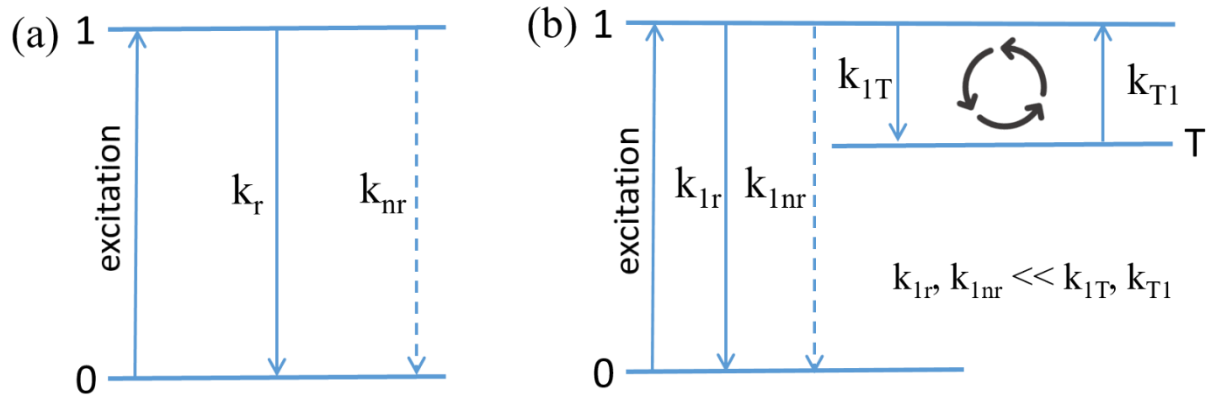

Figure 1. Traditional two-level (a) and delayed luminescence three-level (b) energy diagrams which can be used for phenomenological description of photophysical processes in perovskite nanocrystals; 0, 1 and T are the ground (unexcited), excited (excitonic) and shallow trap states, respectively; k_r and k_{nr} in (a) as well as k_{1r} and k_{1nr} in (b) are the radiative and non-radiative rate constants of the exciton recombination; k_{1T} and k_{T1} are the rate constants of trapping and de-trapping. The black circular arrows in (b) symbolize the cyclic process of population exchange between the bright excitonic and dark trap states.

However, there are experimental facts in perovskite photophysics which principally contradict the two-level diagram presented in Fig. 1a. First of all, based on the extinction coefficients (absorption cross sections) of perovskite nanocrystals of the excitonic optical transition, the radiative lifetime of the perovskite nanocrystals should be of the order of 1 ns or less [6, 7, 10, 11]. Because the non-radiative processes can only shorten the PL decay kinetics as compared to the radiative lifetime, it means that the experimentally measured excitonic PL lifetimes τ_{PL} for perovskite nanocrystals in the framework of the diagram in Fig. 1a should be less or much less than 1 ns. However, the experimentally measured τ_{PL} for 3D perovskite nanocrystals are from a few nanoseconds to several microseconds [6, 7]. Thus, the long lifetimes are not compatible either with the *direct-gap* origin of the perovskite systems or with the *two-level model.*

The above indicated contradiction can be resolved within the framework of our recently proposed scheme for the origin of PL kinetics in perovskite nanoparticles, as illustrated in Fig. 1b [6, 7], which is an analogue of the well-known thermally activated delayed fluorescence in molecular photophysics [12-14]. This is the so-called delayed luminescence model including shallow traps (T in Fig. 1b), which capture and hold the carriers during some time followed by their returning to the emissive (excitonic) state 1. In the framework of the *delayed luminescence model* very long experimentally measured PL lifetimes τ_{PL} of perovskite nanocrystals are well consistent with high radiative rate constants k_{1r} (about 10^9 s^{-1} and higher) typical for direct gap semiconductors. Indeed, as one can see in Fig. 1b, if the delayed luminescence condition $k_{1T} >> k_{1r}$, k_{1nr} is fulfilled, after being excited to the state 1, a majority of photoexcited carriers are preferably trapped with the time constant k_{1T} by the state T, and only small part of them recombine radiatively or non-radiatively with the rate constants k_{1r} and k_{1nr}, respectively. The rate constants for the carrier trapping and de-trapping k_{1T} and k_{T1} are suggested to be related to each other by the expression [6, 7]

$$k_{T1} = k_{1T} \exp(-\Delta E / k_B T) \qquad (3)$$

where ΔE, k_B and T are the energy difference between the emissive and trap states, the Boltzmann coefficient and temperature in Kelvins, respectively. The proposed delayed luminescence scheme easily combines the short times of radiative recombination (high values of the rate constant k_{1r}) and very long decay times τ_{PL} of the experimentally observed photoluminescence.

As an example, let us analyze with the delayed luminescence model the above mentioned PL decay kinetics with the PL decay time τ_{PL} = 25 ns and the PL quantum yield Φ = 1.0. It is important to note that, for such an analysis, it is necessary to know in advance the values of the radiative recombination rate constant k_{1r} as well as the trapping rate constant k_{1T}. For example, We

consider the values of k_{1r}=5·10^8 s^{-1} and k_{1T}=2.5×10^{11} s^{-1}. Since Φ = 1.0, it means that k_{1nr} = 0. Then we have to fit the experimental PL kinetics, exponentially decaying with τ_{PL} = 25 ns, by the differential rate equations (4) and (5), which describe all possible depopulation processes in the scheme in Fig. 1b, with use of ΔE as parameter. We performed such calculations, and the fitting resulted in ΔE ~ 60 meV. Therefore, having the radiative recombination rate as high as k_{1r} = 5·10^8 s^{-1}, the process of multiple trapping and de-trapping by the trap with ΔE ~ 60 meV below the emissive state 1 leads to the PL decay kinetics with the PL lifetime as long as 25 ns.

$$\frac{dn_1}{dt} = -(k_{1r} + k_{1nr})n_1 - k_{1T}n_1 + k_{T1}n_T \quad (4)$$

$$\frac{dn_T}{dt} = k_{1T}n_1 - k_{T1}n_T \quad (5)$$

It is worth to note that the τ_{PL} values may reach even microseconds if the trap state T is sufficiently deep (if ΔE is higher than about 200 meV, see Fig. 2b and Ref. 6).

It is important to recognize that the application of the traditional two-level model to perovskite nanocrystals can result in erroneous conclusions. First of all, this refers to measurements of the excited state quenching constants (hereinafter k_q). For example, if there is some excited state interaction which results in PL lifetime and PLQY decrease from 25 ns to 12.5 ns and from 1.0 to 0.5, respectively, then the quenching rate constant k_q is calculated within the two-level scheme as $k_q = k_{nr} = (25\ \text{ns})^{-1} = 0.04 \cdot 10^9\ \text{s}^{-1}$. However, in the framework of the delayed luminescence model and with the above mentioned parameters, the two-fold decrease of the PL decay time and quantum yield is due to an appearance of the non-radiative recombination channel with $k_{1nr} = k_q = 0.5 \cdot 10^9\ \text{s}^{-1}$, which is one order of magnitude higher than in the case of the two-level model, where the radiative exciton lifetime is clearly inconsistent with its high oscillator strength of the (direct gap) perovskite.

Is there any direct evidence that the delayed luminescence model adequately describes the photophysical behavior of perovskite nanocrystals? We believe that the PL lifetime shortening at low temperatures as compared to the room temperature values, that is predicted by the delayed luminescence model, could be such a proof. Indeed, as we described, at room temperature the PL kinetics of perovskite NCs is formed as a result of the effect of multiple trapping (the rate constant k_{1T}) and de-trapping (the rate constant k_{T1}, which notably increases by increasing T after Eq. 3) by shallow non-quenching traps [6, 7]. Thus, the experimentally observed PL kinetics is in fact determined by the rate constant k_{T1} of de-trapping which strongly decreases (increases) with a decrease (increase) of temperature. At very low temperatures the k_{T1} becomes very small, which means that *all* shallow traps become completely filled by carriers due to illumination. At these conditions carrier trapping becomes impossible. This is equivalent to the absence of the trap states, so that the system can be considered as two-level one (Fig. 1b) for which the simple expression $k_{1r} = 1/\tau_{PL}$ is still valid.

Figure 2. (a) PL decay kinetics of a thin layer of $CsPbBr_{1.5}I_{1.5}$ nanocrystals measured at 15 (1) and 300 K (2) at the PL band maxima (695 and 680 nm, respectively, see the PL spectra in the inset) after excitation at 405 nm by 100 fs pulses (76 MHz pulse repetition rate). Colored lines are experimental data, black solid lines are the results of two-exponential fitting where contributions of short-lived components are more than 99%. Grey filled curve is the instrument response function. (b) Calculated dependence (symbols) of the PL decay time τ_{PL} on the trap state depth ΔE and fitting of the dependence by an exponential function $\tau = a \cdot \exp(\Delta E/b)$ with a = 2.61 ns and b = 32 meV (red line); (b) is adapted with permission from the American Chemical Society [6].

The predicted effect is really observed for perovskite NCs. As an example, Fig. 2 demonstrates a substantial reduction of the PL lifetime for a thin film of $CsPbBr_{1.5}I_{1.5}$ nanocrystals we found when temperature decreases from 300 down to 15 K. The experimentally measured PL decay time τ_{PL} shortens from 1.8 ns at room temperature down to 0.9 ns at 15 K with a significant (about 2-fold) increase in the PL quantum yield. Such behavior of the PL decay kinetics is anti-

intuitive because one usually expects that, if the PLQY grows with a decrease of temperature, it should be due to PL lifetime lengthening as a result of suppression of temperature-induced quenching processes. In other words, at 15 K, persistent photodoping of $CsPbI_xBr_{x-3}$ NCs is realised that modifies the PL decay mechanism from the delayed PL at room temperature to standard two-level deactivation scheme at low T. Note that the PL lifetime shortening with decrease of temperature was not due to (possible) crystal phase transition because the decrease was monotonic over all the temperature interval of 300 – 15K (to be published elsewhere). Similar effect of the PL decay shortening as a result of temperature decrease was recently observed for $CsPbBr_3$ perovskite nanocrystals [15]. Note that the delayed luminescence model has been recently used to describe long-lived PL decay tails in conventional semiconductor quantum dots [16, 17].

Thus, we can conclude that if the experimentally measured PL lifetime of perovskite nanocrystals at room temperature significantly exceeds a value of the order of 1 ns, then this kinetics is formed due to the mechanism of delayed luminescence and can be assigned to a shallow non-emissive (dark) trap state with the energy ΔE below the emissive excitonic state. There is a one-to-one correspondence between ΔE and τ_{PL} values. An example of τ_{PL} dependence on ΔE is shown in Fig. 2b (obtained for $k_{1r}=4.5\cdot10^8$ c^{-1}, $k_{1nr}=0$, $k_{1T}=2.5\times10^{11}$ s^{-1}, adapted from Ref. 6). At ΔE higher than 75 meV the dependence is well described by the expression $\tau_{PL} = a \cdot \exp(\Delta E/b)$ where a = 2.61 ns and b = 0.032 eV.

Note that if the experimentally measured PL decay kinetics is not monoexponential, one can represent it as a sum of several exponentially decaying components and calculate individual ΔE values for each of them by solving the rate equations (4-5). For example, the PL decay kinetics experimentally measured for $MAPbBr_3$ nanocrystals at room temperature in Ref. 6 can be

represented as a sum of three exponents with time constants of 20, 128.5 and 628.5 ns that corresponds to ΔE values of 63, 125, and 177.5 meV, respectively. Of course, such description of shallow trap states by a set of discrete energies is an idealization. More realistic would be a description with use of a certain trap distribution over energy. We suggest that determination of such trap distribution can be possible in case of analysis of complex PL decay kinetics in terms of *lifetime distribution* (instead of a set of discrete lifetimes) calculated by the maximum entropy method [18, 19].

PL decay kinetics in thin perovskite layers

At first glance, it may seem that the PL decay kinetics in thin (hundreds of nanometers) layers of perovskites are extremely difficult to interpret due to the large number of recombination processes, which can take part in their formation. First of all, these are free carrier bulk recombination processes, such as the quasi-monomolecular deep-trap assisted non-radiative recombination, bimolecular radiative recombination, and Auger recombination (at high carrier concentrations). In addition, it is customary in the literature to consider separately the processes of the non-radiative carrier recombination on a layer surfaces. Fortunately, in the case of metal halide perovskite layers the situation turns out to be favorable for the PL kinetics interpretation because the bulk recombination rates are essentially lower than the non-radiative recombination rates on the surface. Due to this, in most cases the PL decay kinetics in perovskite thin polycrystalline layers is determined by the carrier diffusion across the layer thickness to both front and back surfaces followed by the non-radiative recombination on them (see Fig. 3) [20].

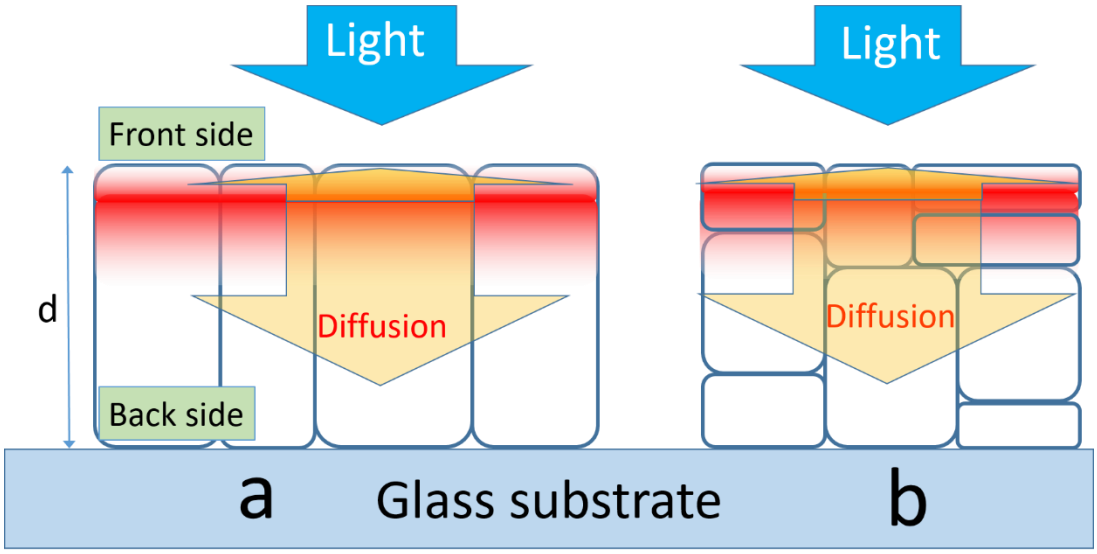

Figure 3. A schematic representation of two possible morphologies of a polycrystalline perovskite layer of thickness d: (a) individual grains occupy the entire thickness of the layer, and (b) several grains stacked on each other form the thickness of the layer. Initial inhomogeneous distribution of photoexcited carriers over the layer thickness formed due to high absorption coefficient of perovskite is shown as a gradient red color. Wide yellow-brown vertical arrows, directed to both the front and back surfaces, show the directions of carrier diffusion across the layer thickness caused by the initial inhomogeneous distribution of carriers and carrier recombination on the surfaces.

Wherein, one should remember that the perovskite layers, which are usually fabricated either by spin coating of precursor solutions (solution-deposited layers) or by vacuum co-deposition of sublimated precursors (vacuum-deposited layers) consist of grains, which are tightly adjacent to each other (see Fig. 3). In principle, one can imagine two possible morphologies of the layers: (a) individual grains occupy the entire thickness of the layer (Fig. 3a), and (b) several grains stacked on each other to form the layer thickness (Fig. 3b). As recent investigations have shown, the boundaries between the grains *inside* the layer do not cause quenching of the PL [21-24] and, therefore, do not participate in the formation of the PL decay kinetics. Only grain boundaries forming *external* surfaces of layer (both front and back surfaces) are usually responsible for the perovskite PL quenching (carrier non-radiative recombination). Numerous data on the significant

(ten-fold and more) lengthening of the PL lifetime in a perovskite layer as a result of chemical passivation of their front surface serve as an evidence of a leading role of the layer surfaces in the PL kinetics formation [25, 26]. Therefore, according to literature data, the most efficient mechanism responsible for carrier recombination in perovskite layers is non-radiative recombination on the layer surfaces. In such a case, from the point of view of extracting maximum of physical information, the most reasonable method of analyzing PL kinetics is fitting them with use of a one-dimensional diffusion equation. It makes possible to obtain simultaneously the values of the carrier ambivalent diffusion coefficient D and the surface recombination velocity S [20].

It should be noted that, generally speaking, the diffusion equation is applicable only for homogeneous materials. It is obvious that polycrystalline perovskite layers are not homogeneous, since they contain not only bulk material, which in the first approximation can be considered the same in different grains, but also grain boundaries. However, in reality, the situation here is quite favorable from the point of view of interpretation of the luminescence kinetics, because after photoexcitation the diffusion moves the charges only in the vertical direction through the layer thickness, since only in this direction there is an initial photoinduced concentration gradient (the gradient is shown by the red color in Fig. 3). Therefore, the morphology presented in Fig. 3a can be considered as homogeneous from the point of view of diffusion across the layer thickness. It is believed in the literature that in most of the state-of-the-art perovskite films are continuous and monocrystalline in the vertical direction [27, 28] (Fig. 3a). However, that the structures shown in Fig. 3b are also possible as in samples prepared by vacuum evaporation or films employed in the fabrication of LEDs where small grain sizes are preferred. In such structures, perovskite layers consist of grains stacking on top of each other and this is a non-homogeneous material because, in course of diffusion, carriers have to cross several internal boundaries to reach the layer surfaces

that can essentially retards the diffusion [29]. Therefore, in case of morphology shown in Fig. 3b the values of D, obtained as a result of the PL kinetics fitting by the diffusion equation, are consequently effective (averaged) values.

Another comment concerns the consideration of the bimolecular recombination of carriers in the layer bulk. As our experience shows, it is reasonable to minimize a contribution of this mechanism to the kinetics because it makes the diffusion equation much more complex and thus decreases the accuracy of determination of D and S values. The bimolecular recombination exclusion can be done by reducing the concentration of photoexcited carriers below a certain value, approximately 10^{17} cm^{-3} [30].

The time dependence of the concentration *n* of photogenerated charge carriers along the layer thickness can be described by the one-dimensional diffusion equation in the following form:

$$\frac{\partial n(x,t)}{\partial t} = D\frac{\partial^2 n(x,t)}{\partial x^2} - \frac{n(x,t)}{\tau_B} + G(x,t) \quad (6)$$

$$G(x,t) \propto I(x,t) \cdot e^{-\alpha x} \quad (7)$$

where D is the diffusion coefficient, τ_B is the bulk carrier lifetime and G (x, t) is the generation rate upon a light pulse, α is the absorption coefficient at the excitation wavelength, and *I(x, t)* is the excitation pulse profile. To solve the equation (6), standard boundary conditions describing recombination on the front (equation 8) and rear (equation 9) surfaces should be also used:

$$\left.\frac{\partial n(x,t)}{\partial x}\right|_{x=0} = \frac{S_F}{D} n(0,t) \quad (8)$$

$$\left.\frac{\partial n(x,t)}{\partial x}\right|_{x=L} = -\frac{S_B}{D} n(d,t) \quad (9)$$

where S_F and S_B are the surface recombination velocity, respectively, on the front and back side, *d* is the layer thickness. The numerical solution of the diffusion equation (6) with conditions (7-9) enables to obtain the distribution of charge carriers over the layer thickness as a function of time. The relationship between the carrier distribution and the experimentally measured kinetics of the PL decay $I_{PL}(t)$ can be done by the equation:

$$I_{PL}(t) = \int_0^L n(x,t)dx \qquad (10)$$

Thus, by fitting an experimental PL decay kinetics $I_{PL}(t)$ with the diffusion equation, one can determine D and S values as fitting parameters. In the literature on perovskites, such a diffusion approach of the PL kinetics interpretation was mainly used to determine the diffusion coefficients for electrons and holes under the conditions of the perovskite surface coating by an electron- or hole-transport layer, respectively [31-33]. Only in few works, this approach was used to determine both parameters, diffusivity D and surface recombination velocity S, with the free surface of the perovskite layer [20].

To fit the experimental kinetics of perovskite layers using equation (6), it is necessary to know the carrier lifetime (luminescence lifetime) in the bulk. It is often impossible to measure this value experimentally because of the quenching effect of the layer surfaces. However, it can be assumed that this value is at least 1 microsecond, since passivating only the front surface of the layer usually extends the luminescence lifetime to several microseconds [25, 26]. In our calculations (see below), we assumed τ_B = 1 μs.

In Fig. 4 we show the results of modeling of the luminescence decay kinetics we performed by solving the diffusion equation (6) for various combinations of D and S (here we neglect bimolecular recombination of carriers and assume τ_B = 1 μs). As one can see, for large values of

D (of the order of 1 cm^2/s and more), the kinetics no longer depend on D and are determined only by the values of S (Fig. 4a and 4b). This means that the diffusion redistribution of carriers over the layer thickness occurs much faster than the carrier recombination on the surface. In this case of very fast diffusion, the PL decay can be fitted with a single exponential, and when $\tau_{PL} << \tau_B$ the relation (11) is valid, which allows one to determine the value of S knowing the experimentally measured PL lifetime τ_{PL} and the layer thickness d [34]:

$$S = \frac{d}{2\tau_{PL}} \tag{11}$$

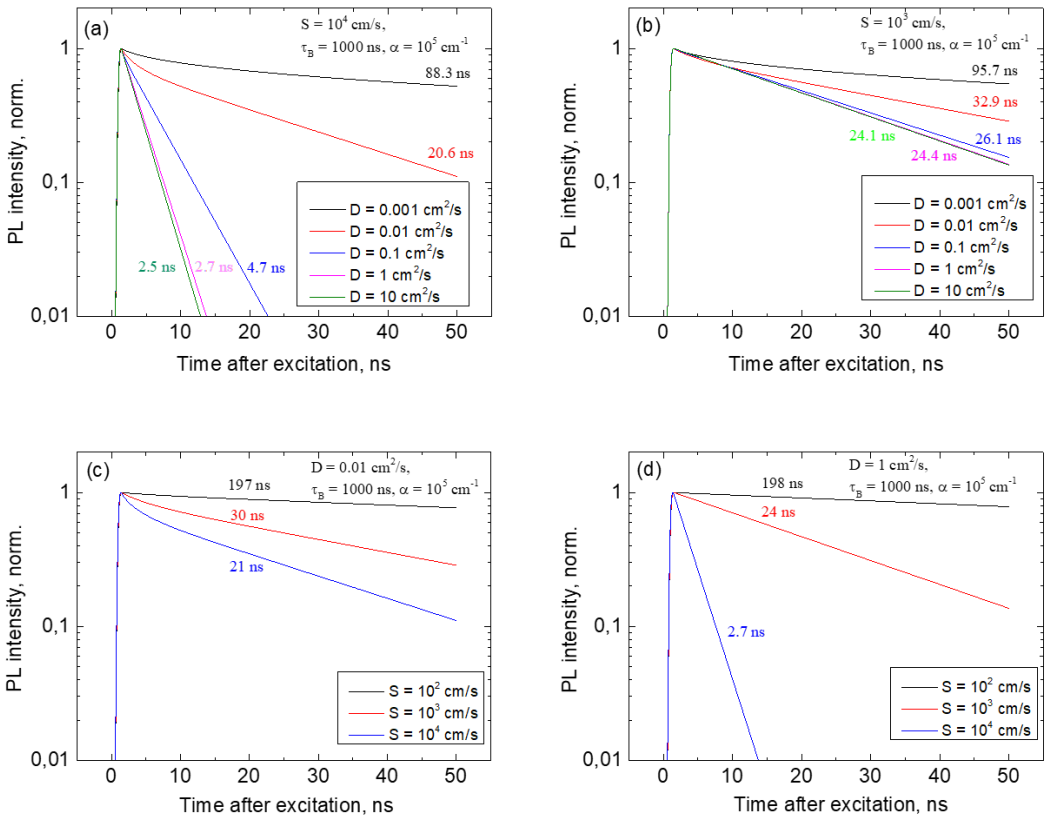

Figure 4. Model PL kinetics calculated by the diffusion equation for different D and S values. In all cases absorption coefficient $\alpha=10^5$ cm^{-1}, τ_B=1000 ns. The model corresponds to the case when bimolecular recombination of carriers is absent ($n \sim 10^{15}$ - 10^{16} cm^{-3}).

It should be noted that the values of D obtained as a result of fitting the luminescence decay kinetics in thin layers of perovskites can provide additional information about the morphology of these layers. Indeed, as the literature data analysis performed in Ref. 35 shows, average carrier mobilities for $CH_3NH_3PbI_3$ perovskite thin films, measured by THz and microwave methods, which are short-range by their origin and inform only about carrier transport inside (sub)micrometer grains, are of μ=37 $cm^2/(V\ s)$ (D=0.93 cm^2/s). This is very close to the average values of μ=73 cm2/(V s) (D=1.8 cm^2/s) found for single crystals [35]. Recent direct measurements by the Light Induced Transient Grating method also showed that the diffusion coefficient of carriers in the plane of the layer at distances less than the grain size is of the same order of 1-2 cm^2/s [36, 37]. Thus, it can be assumed that the transport of carriers inside the individual grains and in the volume of single-crystal perovskites occurs in the same way, with a diffusion coefficient of about 1-2 cm^2/s. Therefore, we assume that if the PL kinetics fitting for the perovskite layers result in such high values of D, this indicates that the morphology shown in Fig. 3a is realized in these layers, when perovskite grains occupy the entire thickness of the layer. In this case, diffusion in the vertical direction occurs only in the bulk material without participation of grain boundaries, as in single crystals of perovskites. If the PL kinetics fitting yields values of D significantly smaller than 1 cm^2/s (see the review [35]), then this is likely an indication that the structure of the perovskite layer is closer to that shown in Fig. 3b.

In conclusion, simple procedures are described in this work for interpretation of the PL decay kinetics of metal halide perovskite structures. In case of well passivated nanocrystals, an application of the delayed luminescence model can give insight into the distribution of small non-quenching (surface) traps responsible for the PL kinetics formation. In case of thin polycrystalline films limited by interfacial recombination, the PL decay fitting by one-dimensional diffusion

equation enables one to determine the diffusivity D and the surface recombination velocity S values and, thus, evaluate qualitatively the layer morphology.

Methods

Synthesis of Colloidal solution. $CsPbBr_{1.5}I_{1.5}$ mixed halideperovskite nanocrystals were prepared by following the hot-injection method [38,39] with some modifications. Firstly, Cs-oleate solution was achieved by mixing under constant stirring 0.410 g of Cs_2CO_3, (99.9 %, Sigma-Aldrich), 1.25 mL of oleic acid (OA, 90 %, Sigma-Aldrich) and 20 mL of 1-octadecene (1-ODE, 90 %, Sigma-Aldrich) into a 50 mL- three neck-flask under vacuum for 1 h. Then, the solution was heated at 150 °C under N_2 atmosphere until dissolve Cs_2CO_3 completely. In order to avoid the precipitation of Cs-oleate, the mixture was stored under N_2, keeping the temperature at 100 °C.

For carrying out the $CsPbBr_{1.5}I_{1.5}$ colloidal solution, 0.346 g $PbBr_2$ (99.999%, ABCR), 0.432 g PbI_2 (99.99%, TCI) and 50 mL de 1-ODE were mixed into a 100 mL-three neck flask and heated at 120 °C for 1 h under vacuum conditions. Then, both OA and oleylamine (5 mL each one) were separately loaded into the halide solution under N_2-purge and quickly heated to reach 170 °C, injecting 4 mL of the preheated Cs-oleate solution immediately. Lastly, the reaction was quenched by adding the flask into an ice bath for 5 s. In order to perform the perovskite isolation process, the as-prepared $CsPbBr_{1.5}I_{1.5}$ colloidal solution was centrifuged at 4700 rpm for 15 min. The nanocrystals pellets were obtained from the supernatant and concentrated to 50 mg mL^{-1} with hexane.

Sample preparation. $CsPbBr_{1.5}I_{1.5}$ perovskite nanocrystals were deposited on a commercial borosilicate substrate by means of spin-coating method with post-baking at 100 ºC for 1 minute. Prior to the deposition substrates were carefully cleaned with acetone, ethanol and isopropanol during 10 minutes in an ultrasound bath.

Low temperature PL and time-resolved PL measurements. Samples were held in a cold finger of a closed-cycle He cryostat, which can be cooled down to 10K. PL was excited by using a Ti:sapphire mode-locked laser (Coherent Mira 900D, 200 fs pulses with a repetition rate 76 MHz) at a wavelength of 405 nm obtained by doubling initial 810 nm emission with a BBO crystal. To measure PL spectra, the PL signal was dispersed by a double 0.3 m focal length grating spectrograph and detected with a back illuminated Si CCD. To measure PL transients, the emitted light is collected on a Si avalanche photodiode connected to a time correlated single photon counting electronics.

PL kinetics modeling. The numerical solution of the differential equation was made in the framework of the Crank-Nicolson difference scheme.

Acknowledgements

Financial support by Spanish MINECO through project nº TEC2017-86102-C2-1-R, the European Research Council (ERC) via Consolidator Grant (724424 - No-LIMIT) and and Generalitat Valenciana via Prometeo Grant Q-Devices (Prometeo/2018/098) are gratefully acknowledged. J.N. Arenas acknowledges MINECO for the support through FPI Fellowship Program (XXXX).

References

1. W. Rehman, R. L Milot, G. E. Eperon; C. Wehrenfennig, J. L. Boland, H. J. Snaith, M. B. Johnston, L. M. Herz, Charge-carrier dynamics and mobilities in formamidinium lead mixed-halide perovskites. Adv. Mater. 27 (2015) 7938-7944. https://doi.org/10.1002/adma.201502969

2. J. Borchert, R. L. Milot, J. B. Patel, C. L. Davies, A. D. Wright, L. Martínez Maestro, H. J. Snaith, L. M. Herz, M. B. Johnston, Large-Area, Highly Uniform Evaporated Formamidinium Lead Triiodide Thin Films for Solar Cells, ACS Energy Lett. 2 (2017) 2799-2804. https://doi.org/10.1021/acsenergylett.7b00967

3. I. Levine, S. Gupta, A. Bera, D. Ceratti, G. Hodes, D. Cahen, D. Guo, T. J. Savenije, J. Ávila, H. J. Bolink, O. Millo, D. Azulay, I. Balberg, Can we use time-resolved measurements to get steady-state transport data for halide perovskites? J. Appl. Phys. 124 (2018) 103103. https://doi.org/10.1063/1.5037637

4. I. L. Braly, D. W. deQuilettes, L. M. Pazos-Outón, S. Burke, M. E. Ziffer, D. S. Ginger, H. W. Hillhouse, Hybrid perovskite films approaching the radiative limit with over 90% photoluminescence quantum efficiency. Nat. Photonics 12 (2018) 355-361. https://doi.org/10.1038/s41566-018-0154-z

5. H. Huang, A. S. Susha; S. V. Kershaw, T. F. Hung, A. L. Rogach, Control of emission color of high quantum yield CH3NH3PbBr3 perovskite quantum dots by precipitation temperature. Adv. Sci. 2 (2015) 1500194. https://doi.org/10.1002/advs.201500194

6. V. S. Chirvony, S. González-Carrero, I. Suárez, R. E. Galian, M. Sessolo, H. J. Bolink, J. P. Martínez-Pastor, J. Pérez-Prieto, Delayed luminescence in lead halide perovskite nanocrystals, J. Phys.Chem. C 121 (2017) 13381-13390. https://doi.org/10.1021/acs.jpcc.7b03771

7. V. S. Chirvony, J. P. Martínez-Pastor, Trap-Limited Dynamics of Excited Carriers and Interpretation of the Photoluminescence Decay Kinetics in Metal Halide Perovskites, J. Phys. Chem. Lett. 9 (2018) 4955-4962. https://doi.org/10.1021/acs.jpclett.8b01241

8. H. Diab, C. Arnold, F. Lédée, G. Trippé-Allard, G. Delport, C. Vilar, F. Bretenaker, J. Barjon, J.-S. Lauret, E. Deleporte, D. Garrot, Impact of Reabsorption on the Emission Spectra and Recombination Dynamics of Hybrid Perovskite Single Crystals, J. Phys. Chem. Lett. 8 (2017) 2977-2983. https://doi.org/10.1021/acs.jpclett.7b00998

9. D. Hong, J. Li, S. Wan, I. G. Scheblykin, Y. Tian, Red-Shifted Photoluminescence from Crystal Edges Due to Carrier Redistribution and Reabsorption in Lead Triiodide Perovskites, J. Phys. Chem. C 123 (2019) 12521-12526. https://doi.org/10.1021/acs.jpcc.9b03647

10. K. Gong, Y. Zeng, D. F. Kelley, Extinction coefficients, oscillator strengths, and radiative lifetimes of CdSe, CdTe, and CdTe/CdSe nanocrystals, J. Phys. Chem. C 117 (2013) 20268-20279. https://doi.org/10.1021/jp4065449

11. J. Maes, L. Balcaen, E. Drijvers, Q. Zhao, J. De Roo, A. Vantomme, F. Vanhaecke, P. Geiregat, Z. Hens, Light absorption coefficient of $CsPbBr_3$ perovskite nanocrystals, J. Phys. Chem. Lett. 9 (2018) 3093-3097. https://doi.org/10.1021/acs.jpclett.8b01065

12. A. M. Kelley, Condensed-Phase Molecular Spectroscopy and Photophysics; Wiley: Hoboken, NJ, 2013.

13. Q. Zhang, B. Li, S. Huang; H. Nomura, H. Tanaka, C. Adachi, Efficient blue organic light-emitting diodes employing thermally activated delayed fluorescence, Nat. Photonics 8 (2014) 326-332. https://doi.org/10.1038/nphoton.2014.12

14. S. M. Bachilo, A. F. Benedetto, R. B. Weisman, J. R. Nossal, W. E. Billups, Time-resolved thermally activated delayed fluorescence in C_{70} and 1,2-$C_{70}H_2$, J. Phys. Chem. A 104 (2000) 11265-11269. https://pubs.acs.org/doi/10.1021/jp002742k

15. F. Gabelloni, F. Biccari, G. Andreotti, D. Balestri, S. Checcucci, A. Milanesi, N. Calisi, S. Caporali, A. Vinattieri, Recombination dynamics in CsPbBr3 nanocrystals: role of surface states. Opt. Mater. Express 7 (2017) 4367-4373. https://doi.org/10.1364/OME.7.004367

16. P. J. Whitham, A. Marchioro, K. E. Knowles, T. B. Kilburn, P. J. Reid, D. R. Gamelin, Single-particle photoluminescence spectra, blinking, and delayed luminescence of colloidal CuInS2 nanocrystals. J. Phys. Chem. C 120 (2016) 17136-17142. pubs.acs.org/doi/abs/10.1021/acs.jpcc.6b06425

17. F. T. Rabouw, J. C. van der Bok, P. Spinicelli, B. Mahler, M. Nasilowski, S. Pedetti, B. Dubertret, D. Vanmaekelbergh, Temporary charge carrier separation dominates the photoluminescence decay dynamics of colloidal CdSe nanoplatelets. Nano Lett. 16 (2016) 2047-2053. https://pubs.acs.org/doi/abs/10.1021/acs.nanolett.6b00053

18. A. A. Maskevich, V. I. Stsiapura, P. T. Balinski. Analysis of fluorescence decay kinetics of thioflavin by a maximum entropy method. J. Appl. Spectroscopy, 77 (2010) 194-201. https://doi.org/10.1007/s10812-010-9314-8

19. K. Virkki, S. Demir, H. Lemmetyinen, and N. V. Tkachenko, Photoinduced Electron Transfer in CdSe/ZnS Quantum Dot-Fullerene Hybrids, J. Phys. Chem. C 119 (2015) 17561-17572. https://doi.org/10.1021/acs.jpcc.5b04251

20. Y. Yang, M. Yang, D. T. Moore, Y. Yan, E. M. Miller, K. Zhu, M. C. Beard, Top and bottom surfaces limit carrier lifetime in lead iodide perovskite films, Nat. Energy 2 (2017) 16207. https://doi.org/10.1038/nenergy.2016.207

21. R. Ciesielski, F. Schäfer, N. F. Hartmann, N. Giesbrecht, T. Bein, P. Docampo, A. Hartschuh, Grain Boundaries Act as Solid Walls for Charge Carrier Diffusion in Large Crystal MAPI Thin Films, ACS Appl. Mater. Interfaces 10 (2018) 7974-7981. https://doi.org/10.1021/acsami.7b17938

22. M. Yang, Y. Zeng, Z. Li, D. H. Kim, C.-S. Jiang, J. van de Lagemaat, K. Zhu, Do grain boundaries dominate non-radiative recombination in CH3NH3PbI3 perovskite thin films? Phys. Chem. Chem. Phys. 19 (2017) 5043-5050. https://doi.org/10.1039/c6cp08770a

23. W. Tian, C. Zhao, J. Leng, R. Cui, S. Jin, Visualizing Carrier Diffusion in Individual Single-Crystal Organolead Halide Perovskite Nanowires and Nanoplates. J. Am. Chem. Soc. 137 (2015) 12458-12461. https://pubs.acs.org/doi/10.1021/jacs.5b08045

24. C. Zhao, W. Tian, J. Leng, R. Cui, W. Liu, S. Jin, Diffusion correlated local photoluminescence kinetics in CH3NH3PbI3 perovskite single-crystalline particles. Sci. Bull. 61 (2016) 665-669. https://doi.org/10.1007/s11434-016-1036-8

25. I. L. Braly, D. W. deQuilettes, L. M. Pazos-Outón, S. Burke, M. E. Ziffer, D. S. Ginger, H. W. Hillhouse, Hybrid perovskite films approaching the radiative limit with over 90%

photoluminescence quantum efficiency. Nat. Photonics 12 (2018) 355–361. https://doi.org/10.1038/s41566-018-0154-z

26. D. W. deQuilettes, S. Koch, S. Burke, R. K. Paranji, A. J. Shropshire, M. E. Ziffer, D. S. Ginger, Photoluminescence Lifetimes Exceeding 8 μs and Quantum Yields Exceeding 30% in Hybrid Perovskite Thin Films by Ligand Passivation. ACS Energy Lett. 1 (2016) 438-444. https://doi.org/10.1021/acsenergylett.6b00236

27. N. Giesbrecht, J. Schlipf, L. Oesinghaus, A. Binek, T. Bein, P. Müller-Buschbaum, P. Docampo, Synthesis of Perfectly Oriented and Micrometer-Sized MAPbBr3 Perovskite Crystals for Thin-Film Photovoltaic Applications. ACS Energy Lett. 1 (2016)150-154. https://pubs.acs.org/doi/10.1021/acsenergylett.6b00050

28 N. Giesbrecht, J. Schlipf, I. Grill, P. Rieder, V. Dyakonov, T. Bein, A. Hartschuh, P. Müller-Buschbaum, P. Docampo, Single-Crystal-Like OptoelectronicProperties of MAPbI3 Perovskite Polycrystalline Thin Films. J. Mater. Chem. A 6 (2018) 4822-4828. https://doi.org/10.1039/C7TA11190H

29. R. Ciesielski, F. Schäfer, N. F. Hartmann, N. Giesbrecht, T. Bein, P. Docampo, A. Hartschuh, Grain Boundaries Act as Solid Walls for Charge Carrier Diffusion in Large Crystal MAPI Thin Films, ACS Appl. Mater. Interfaces 19 (2018) 7974-7981. https://pubs.acs.org/doi/abs/10.1021/acsami.7b17938

30. J. Kim, R. Godin, S. D. Dimitrov, T. Du, D. Bryant, M. A. McLachlan, J. R. Durrant, Excitation Density Dependent PhotoluminescenceQuenching and Charge Transfer Efficiencies in Hybrid Perovskite/Organic Semiconductor Bilayers, Adv. Energy Mater. 8 (2018) 1802474. https://doi.org/10.1002/aenm.201802474

31. S. D. Stranks, G. E. Eperon, G. Grancini, C. Menelaou, M. J. P. Alcocer, T. Leijtens, L. M. Herz, A. Petrozza, H. J. Snaith, Electron-Hole Diffusion Lengths Exceeding 1 Micrometer in an Organometal Trihalide Perovskite Absorber, Science 342 (2013) 341-344. https://doi.org/10.1126/science.1243982

32. G. Xing, N. Mathews, S. Sun, S. S. Lim, Y. M. Lam, M. Gratzel, S. Mhaisalkar, T. C. Sum, Long-Range Balanced Electron- and Hole-Transport Lengths in Organic-Inorganic $CH_3NH_3PbI_3$, Science 342 (2013) 344-347. https://doi.org/10.1126/science.1243167

33. F. Xie, H. Su, J. Mao, K. S. Wong, W. C. H. Choy, Evolution of Diffusion Length and Trap State Induced by Chloride in Perovskite Solar Cell, J. Phys. Chem. C 120 (2016) 21248-21253. https://doi.org/10.1021/acs.jpcc.6b06914

34. A. B. Sproul, Dimensionless solution of the equation describing the effect of surface recombination on carrier decay in semiconductors, J. Appl. Phys. 76 (1994) 2851-2854. https://doi.org/10.1063/1.357521

35. L. M. Herz, Charge-Carrier Mobilities in Metal Halide Perovskites: Fundamental Mechanisms and Limits, ACS Energy Lett. 2 (2017) 1539-1548. https://pubs.acs.org/doi/10.1021/acsenergylett.7b00276

36. D. H. Arias, D. T. Moore, J. van de Lagemaat, J. C. Johnson, Direct Measurements of Carrier Transport in Polycrystalline Methylammonium Lead Iodide Perovskite Films with Transient Grating Spectroscopy, J. Phys. Chem. Lett. 9 (2018) 5710-5717. https://doi.org/10.1021/acs.jpclett.8b02245

37. D. Webber, C. Clegg, A. W. Mason, S. A. March, I. G. Hill, K. C. Hall, Carrier Diffusion in Thin-Film $CH_3NH_3PbI_3$ Perovskite Measured using Four-wave Mixing. Appl. Phys. Lett. 111 (2017) 121905. https://doi.org/10.1063/1.4989970.

38. L. Protesescu, S. Yakunin, M. I. Bodnarchuk, F. Krieg, R. Caputo, C. H. Hendon, R. X. Yang, A. Walsh, M. V. Kovalenko, Nanocrystals of Cesium Lead Halide Perovskites (CsPbX3 , X = Cl, Br, and I): Novel Optoelectronic Materials Showing Bright Emission with Wide Color Gamut, Nano Lett. 15 (2015) 3692-3696. https://pubs.acs.org/doi/10.1021/nl5048779